

PTEN Inhibition Improves Muscle Regeneration in Mice Fed a High-Fat Diet

Zhaoyong Hu,¹ Huiling Wang,² In Hee Lee,¹ Swati Modi,¹ Xiaonan Wang,³ Jie Du,¹ and William E. Mitch¹

OBJECTIVE—Mechanisms impairing wound healing in diabetes are poorly understood. To identify mechanisms, we induced insulin resistance by chronically feeding mice a high-fat diet (HFD). We also examined the regulation of phosphatidylinositol 3,4,5-trisphosphate (PIP₃) during muscle regeneration because augmented IGF-1 signaling can improve muscle regeneration.

RESEARCH DESIGN AND METHODS—Muscle regeneration was induced by cardiotoxin injury, and we evaluated satellite cell activation and muscle maturation in HFD-fed mice. We also measured PIP₃ and the enzymes regulating its level, IRS-1-associated phosphatidylinositol 3-kinase (PI3K) and PTEN. Using primary cultures of muscle, we examined how fatty acids affect PTEN expression and how PTEN knockout influences muscle growth. Mice with muscle-specific PTEN knockout were used to examine how the HFD changes muscle regeneration.

RESULTS—The HFD raised circulating fatty acids and impaired the growth of regenerating myofibers while delaying myofiber maturation and increasing collagen deposition. These changes were independent of impaired proliferation of muscle progenitor or satellite cells but were principally related to increased expression of PTEN, which reduced PIP₃ in muscle. In cultured muscle cells, palmitate directly stimulated PTEN expression and reduced cell growth. Knocking out PTEN restored cell growth. In mice, muscle-specific PTEN knockout improved the defects in muscle repair induced by HFD.

CONCLUSIONS—Insulin resistance impairs muscle regeneration by preventing myofiber maturation. The mechanism involves fatty acid-stimulated PTEN expression, which lowers muscle PIP₃. If similar pathways occur in diabetic patients, therapeutic strategies directed at improving the repair of damaged muscle could include suppression of PTEN activity. *Diabetes* 59:1312–1320, 2010

Impaired healing of injured muscles and delayed recovery following muscle infarction are serious complications of diabetes. Because there is evidence that overexpression of an IGF-1 isoform in muscle (mIGF-1) hastens the repair of injured muscles, defects in insulin/IGF-1 signaling could underlie the poor healing of injured muscles that is associated with diabetes (1). For example, Vignaud et al. (2) reported that streptozotocin-

induced diabetes impairs the regenerative capacity of injured muscles, but the underlying mechanism is obscure. An initial step in the repair of injured muscle involves muscle progenitor or satellite cells, which are activated to proliferate, differentiate, and mature, forming new myofibers (3). During muscle regeneration, these different functions can be identified as increases in the expression of muscle-restricted transcription factors including myogenic determination factor (MyoD), myogenin, and myf5, representing proliferation, differentiation, and maturation, respectively. Ultimately, satellite cells generate new myotubes that combine with existing myofibers to repair damaged muscle (3–5).

Regarding the influence of impaired insulin/IGF-1 signaling in the repair of injured muscle, overexpression of mIGF-1 accelerates muscle repair in models of muscular dystrophies and can prevent the muscle atrophy induced by senescence or excess angiotensin II (6–9). In these conditions, mIGF-1 is beneficial presumably because IGF-1 activates IRS-1-associated phosphatidylinositol 3-kinase (PI3K) activity to produce more phosphatidylinositol 3,4,5-trisphosphate (PIP₃). Subsequently, PIP₃ activates cellular signaling pathways including phosphorylation of Akt (p-Akt) and downstream products involved in muscle growth such as ribosomal protein S6 kinase (S6K1) (10,11). The muscle level of PIP₃ can also be raised if activity of the phosphatase and tensin homolog deleted from chromosome 10 (PTEN) is suppressed. The influence of diabetes on PTEN is not predictable, however, because we found that PTEN expression in muscle of streptozotocin-induced acute diabetes was decreased, whereas in muscles of *db/db* mice it was increased, contributing to variations in muscle PIP₃ levels (12).

To probe the mechanisms underlying the impaired healing of injured muscles associated with diabetes, we investigated the role of PTEN in a model of insulin resistance: prolonged feeding of a high-fat diet (HFD). To study muscle regeneration, we used a standard model of muscle regeneration: injection of cardiotoxin into the tibialis anterior muscle (9,11,13). This procedure causes muscle necrosis and activates muscle satellite cells to proliferate, differentiate, and mature into myofibers (3,13). We found that the response to muscle injury in HFD mice was impaired, as demonstrated by decreased myofiber growth and increased collagen deposition. We also found evidence that fatty acids directly stimulate PTEN expression in muscle cells, so we evaluated the influence of PTEN on muscle regeneration by creating mice with muscle-specific PTEN knockout (MPKO). Our results suggest that manipulation of PTEN activity might be a target for strategies aimed at improving muscle repair in diabetic patients.

From the ¹Nephrology Division, Baylor College of Medicine, Houston, Texas; the ²Nephrology Division, Jimin Hospital, Shanghai, China; and the ³Renal Division, Emory University School of Medicine, Atlanta, Georgia.

Corresponding author: Zhaoyong Hu, zhaoyonh@bcm.edu.

Received 4 August 2009 and accepted 19 February 2010. Published ahead of print at <http://diabetes.diabetesjournals.org> on 3 March 2010. DOI: 10.2337/db09-1155.

© 2010 by the American Diabetes Association. Readers may use this article as long as the work is properly cited, the use is educational and not for profit, and the work is not altered. See <http://creativecommons.org/licenses/by-nc-nd/3.0/> for details.

The costs of publication of this article were defrayed in part by the payment of page charges. This article must therefore be hereby marked "advertisement" in accordance with 18 U.S.C. Section 1734 solely to indicate this fact.

RESEARCH DESIGN AND METHODS

Studies of C57BL/6 mice (The Jackson Laboratories, Bar Harbor, ME) were initiated at ~6 weeks of age. For the subsequent 8 months, mice were fed rodent normal diet (23% protein, 10% fat, and 49% carbohydrate) or a HFD diet (23% protein, 35.8% fat, and 35.5% carbohydrate) (Research Diets, New Brunswick, NJ) (14). All experiments were approved by the Baylor Institutional Animal Care and Use Committee (IACUC). Food was removed at 9:00 A.M., and 6 h later arterial blood from anesthetized mice was obtained to measure blood glucose using the Accu-CHEK Advantage blood glucose meter (Accu-CHEK; Indianapolis, IN). Free fatty acids and insulin were measured in plasma samples using a NEFA kit (Biovision; Mountainview, CA) and the Insulin Immunoassay 1–2–3 kit (American Laboratories, Windham, NH).

Mouse model of skeletal muscle regeneration. We studied a standard model of muscle regeneration (13). The tibialis anterior muscle of anesthetized mice (12 mg/kg xylazine and 60 mg/kg ketamine) was injected with 30 μ l of 10 μ mol/l cardiotoxin from *Naja nigricollis* venom (EMD Biosciences, La Jolla, CA). Cardiotoxin was 95% pure and reproducibly induced a pattern of muscle regeneration (supplemental Fig. 1A, available in an online appendix [http://diabetes.diabetesjournals.org/cgi/content/full/db09-1155/DC1]) (5). The contralateral, control tibialis anterior muscle was injected with 30 μ l PBS. On days 3, 6, 12, 21, and 28 postinjury, mice were anesthetized and tibialis anterior muscles were removed; cryosections (Cryosection Media; Fisher, Pittsburg, PA) were obtained or muscles were frozen in liquid nitrogen and stored at -80°C . Tibias were dissected, and their length was measured by a micrometer; the length was used to factor muscle weights.

MPKO. To generate MPKO mice, we mated *Pten*^{lox/lox} mice (The Jackson Laboratories) with mice expressing the *Cre* transgene under the control of the muscle creatine kinase promoter (15). *Pten*^{lox/-} *Cre*⁺ mice were backcrossed to obtain *Pten*^{lox/lox} *Cre*⁺ offspring (MPKO mice) and littermate control mice, *Pten*^{lox/lox} *Cre*⁻ (referred to as lox/lox) mice. MPKO mice are fertile and gain body and muscle weights normally. MPKO and lox/lox mice were fed the HFD beginning at the age of 4 weeks and studied 8 months later.

Muscle histology. Muscles were obtained from fed mice following anesthesia. Tibialis anterior muscles placed in cryo-molds with embedding media (Fisher, Pittsburgh, PA) were frozen in dry ice/isopentane. Sections were stained with hematoxylin-eosin or Sirius red (16). For immunostaining, sections were fixed at -20°C for 15 min before washing with PBS. Slides were incubated overnight at 4°C with primary antibodies: anti-PTEN (Cell Signaling, Cambridge, MA), anti-PIP₃ (Echelon Biosciences, Salt Lake City, UT), anti-laminin (Sigma-Aldrich, St. Louis, MO), and anti-dystrophin (Santa Cruz Biotechniques, Santa Cruz, CA). Secondary antibodies (Alexafluor; Invitrogen, Carlsbad, CA) were subsequently applied for 30 min at room temperature; nuclei were stained with DAPI (Vector, Burlingame, CA). Sirius red staining was visualized by circularly polarized light. Image capture and quantification were processed using NIS-Elements software (Nikon, Melville, NY). To assess the size distribution of regenerating myofibers, the sizes of ~200 myofibers from each tibialis anterior muscle were analyzed using the NIS-Elements software. The pattern of size distribution was confirmed in at least three mice with each condition.

Cell culture. We isolated myocytes from PTEN (lox/lox) mice fed the control diet and cultured them in Dulbecco's Modified Eagle's Medium/F-10 plus 20% FBS, 2.5 ng/ml Fibroblast Growth Factor (FGF), 4.5 g/l glucose, 100 units/ml penicillin, 100 μ g/ml streptomycin, and 4 mmol/l glutamine as previously described (9,12). At 90% confluence, cells were differentiated into myotubes by switching to Dulbecco's Modified Eagle's Medium containing 2% house serum for 48 h. Myotubes were infected with an adenovirus encoding β -galactosidase (Ad- β -Gal), the control, or Cre recombinase (Ad-Cre) to knockout PTEN. After 24 h, myotubes were treated with palmitate (final concentration 0.2 mmol/l) for an additional 24 h. The efficiency of PTEN knockout was verified by Western blot. The diameter at different sites in individual myotubes was measured three times; 200 myotubes from each group were evaluated in each group (100 \times magnification) using ImageJ software (NIH, Frederick, MD). Each experiment was repeated three times.

Western blot analysis. Tibialis anterior muscles from fed, anesthetized mice were homogenized in tubes in cold radioimmunoprecipitation assay buffer and incubated on ice for 1 h. After centrifugation for 30 min (16,000g), supernatant proteins were separated on 4–20% SDS-PAGE gel (Invitrogen). Primary antibodies (Cell Signaling, Beverly, MA) included anti-PTEN (1:1,000), anti-Akt, anti-phospho-(Ser473)Akt, anti-S6K1, and anti-phospho-(Thr389)S6K1. Anti-desmin and anti-glyceraldehyde-3-phosphate dehydrogenase (GAPDH) were from Santa Cruz Biotechniques. GAPDH was used as a loading control.

IRS-1-associated PI3K activity. Tibialis anterior muscles from fed, anesthetized mice (~30 mg) were homogenized for 5 min in 0.6 ml buffer (137 mmol/l NaCl, 20 mmol/l Tris-HCl [pH 7.4], 1 mmol/l CaCl₂, 1 mmol/l MgCl₂, 0.1 mmol/l Na₂VO₄, 2 μ g/ml leupeptin, 2 μ g/ml aprotinin, 1 mmol/l phenylmethylsulfonyl fluoride, and 1% Nonidet-P40). After incubating on ice for 30 min,

the samples were centrifuged at 13,000g for 10 min and the supernatant (~2 mg protein) was immunoprecipitated overnight at 4°C with 2 μ g anti-IRS-1 antibody (Millipore, Billerica, MA). The precipitate was washed three times with the homogenization buffer and then three times with TNE buffer (20 mmol/l Tris-HCl [pH 7.4], 100 mmol/l NaCl, and 0.5 mmol/l EGTA). PI3K activity was measured as previously described (12).

Measurement of PIP₃ in muscle. PIP₃ was measured as previously described (12). Briefly, 30 mg of fresh tibialis anterior muscle from fed, anesthetized mice was homogenized in 1 ml of 1:1 methanol:chloroform plus 50 μ l of 12 N HCl. After centrifuging (16,000g for 10 min), the organic phase was dried under vacuum, the residue was suspended in 40 μ l chloroform, and phospholipids were separated on activated thin-layer chromatography (TLC) plates (Sigma-Aldrich) using 7:10:1.5:2.5 chloroform:methanol:ammonium hydroxide:water over 3 h. After drying, TLC plates were treated with Odyssey Blocking Solution (Li-Cor, Lincoln, NE) for 30 min and probed overnight with an anti-PIP₃ monoclonal antibody (Echelon). IRDye 800 CW rabbit anti-mouse secondary antibody (Li-Cor) was incubated with TLC plates for 1 h at room temperature and scanned with the Odyssey system (Li-Cor).

Quantitative RT-PCR. Total RNA was isolated using Tri Reagent (Invitrogen), and 2 μ g was used in the reverse transcription reaction; RT-PCR was performed with SYBR Green PCR reagents (Bio-Rad, Hercules, CA) and the Opticon DNA Engine (Bio-Rad) as previously described (12). Primers were as follows: mouse MyoD, forward 5'-ACG ACT GCT TTC ACC ACT CCT-3' and reverse 5'-TCG TCT TAA CTT TCT GCC ACT CCG-3'; mouse myogenin, forward 5'-ACA GCA TCA CGG TGG AGG ATA TGT-3' and reverse 5'-CCC TGC TAC AGA AGT GAT GGC TTT-3'; and mouse GAPDH, forward 5'-ACC CCC AAT GTA T CC GTT GT-3' and reverse 5'-TAC TCC TTG GAG GCC ATG TA-3'.

Statistical analysis. Results are means \pm SE. Differences between the two groups were analyzed by Student's *t* test; multiple comparisons were analyzed by ANOVA with a post hoc analysis by the Student-Newman-Keuls test for multiple comparisons; $P < 0.05$ was considered statistically significant.

RESULTS

HFD suppresses the repair of injured skeletal muscles. Mice fed the HFD for 8 months had significantly greater weight gain and higher blood glucose concentrations than mice fed the normal diet (212.5 ± 14.2 vs. 126.8 ± 8.2 mg/dl for HFD and normal diet, respectively; $P < 0.01$; $n = 12$) (supplemental Fig. 1B). HFD mice also had higher plasma free fatty acid concentrations (1.52 ± 0.12 vs. 0.51 ± 0.17 μ mol/l; $P < 0.01$; $n = 12$) and plasma insulin levels (1.72 ± 0.48 vs. 0.63 ± 0.14 ng/ml; $P < 0.01$; $n = 12$).

The HFD impaired regeneration of injured muscles: the weights of injured tibialis anterior muscles factored for tibia length were significantly lower than values from the mice fed a normal diet (Fig. 1A). On day 6 after injury, the sizes of regenerating myofibers (i.e., those with central nuclei) in muscles of HFD mice were smaller compared with values in mice fed the normal diet. At 12 and 21 days after injury, this pattern persisted (Fig. 1B; supplemental Fig. 1C).

Because a high glucose concentration can stimulate the production of collagen in muscle (17), we stained injured muscles with Sirius red to assess whether collagen accumulates in regenerating muscle of mice fed the HFD. At 12 and 21 days after injury, more collagen was present in muscles of HFD mice compared with results from muscles of mice fed the normal diet (Fig. 1C); the area containing collagen was ~2.5-fold greater in injured muscle of HFD mice compared with results from mice fed the normal diet. Thus, the HFD not only impaired the maturation of myofibers but also stimulated collagen deposition and fibrosis in regenerating muscle.

HFD impairs myofiber maturation but not satellite cell activation in regenerating muscle. Potential causes for delayed regeneration of injured tibialis anterior muscles associated with the HFD include suppression of satellite cell activation or proliferation plus impaired

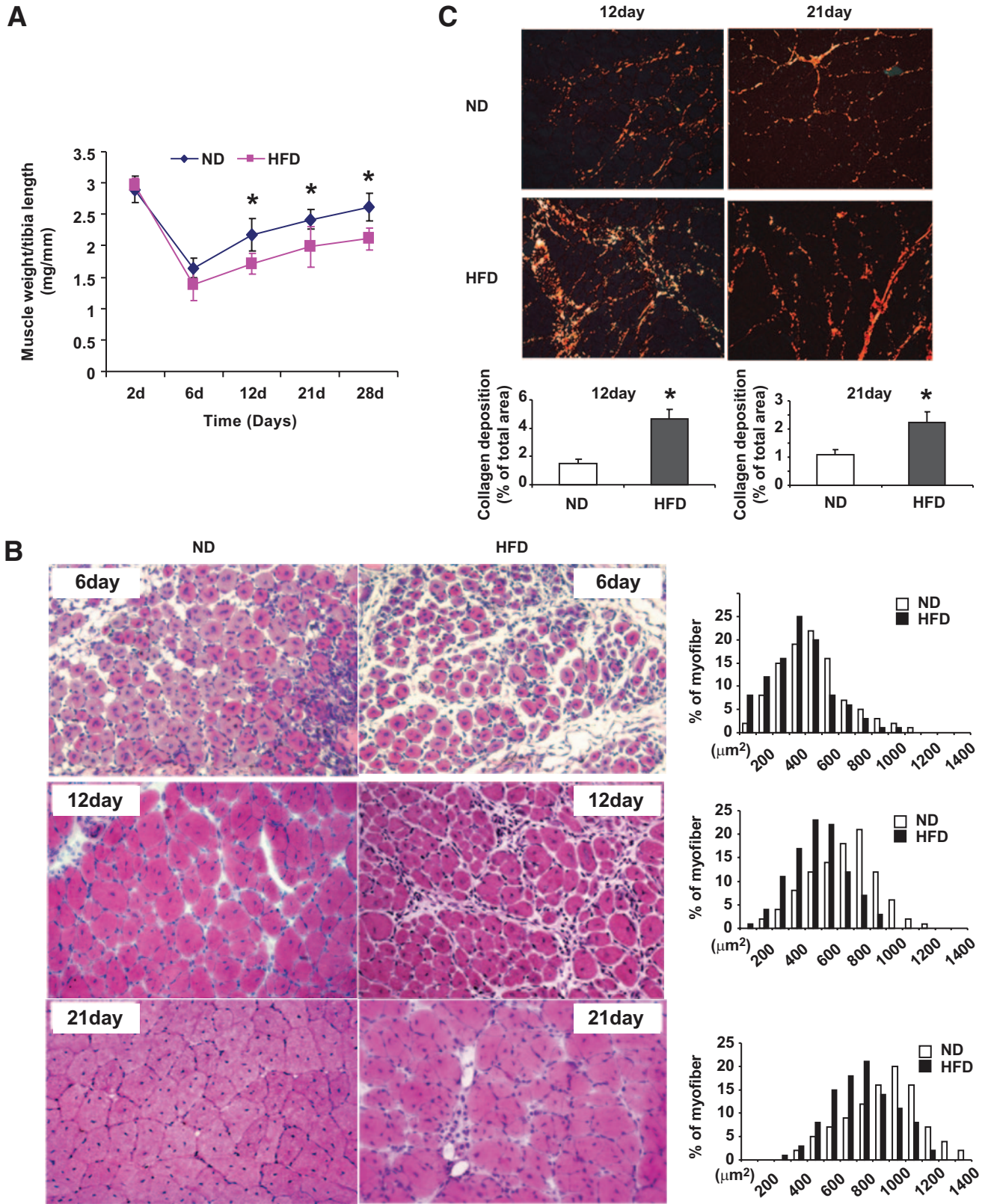


FIG. 1. An HFD delays the recovery of and increases fibrosis in regenerating muscle. **A:** The weights of injured tibialis anterior muscles (normalized to the length of the tibia) were decreased in mice fed the HFD for 8 months. Muscles were obtained at 6, 12, 21, and 28 days after injury and compared with results from mice fed the normal diet (ND). $n = 12$ in each group. **B:** Hematoxylin-eosin sections of injured tibialis anterior muscles from HFD (*right panel*) and normal diet (*left panel*) mice revealed smaller regenerating myofibers (detected by their central nuclei). There also was an increase in interstitial space of muscle. The distribution of cross-sectional areas of new myofibers was shifted leftwards compared with values in mice fed a normal diet. **C:** Sirius red staining revealed an increase in collagen deposition at 12 (*left panel*) and 21 (*right panel*) days after injury in HFD mice. The collagen-containing area was significantly increased in muscles of HFD mice compared with results from muscles of mice on a normal diet ($n = 6$ in each group). $*P < 0.01$. d, days. (A high-quality digital representation of this figure is available in the online issue.)

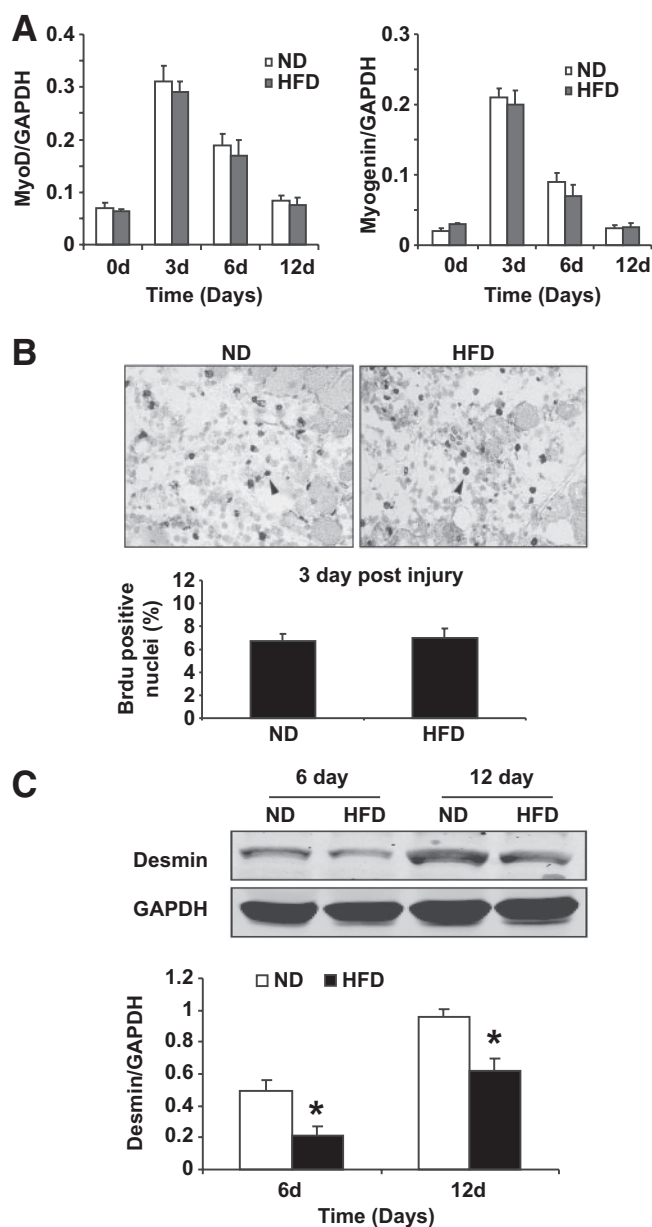


FIG. 2. An HFD suppresses maturation of myofibers in regenerating muscle. **A:** The mRNAs of MyoD or myogenin (markers of satellite cell proliferation) in injured muscles of mice fed the HFD were no different from those in mice fed the normal diet (ND) at days 3 and 6 after injury ($n = 6$ in each group). **B:** Cell proliferation at day 3 after injury was assessed by measuring Brdu incorporation. Arrows indicated typical Brdu-positive nuclei. There were no statistical differences in values from HFD (right panel) and normal diet (left panel) mice ($n = 6$ in each group). **d, days.** **C:** At day 6 and 12 after injury, Western blotting revealed significantly decreased desmin expression in muscles of HFD mice ($n = 6$ in each group of mice) * $P < 0.05$). **d, days.**

differentiation of myoblasts (3). At days 3 and 6 after injury, there was a trend toward lower MyoD and myogenin mRNAs (markers of the activation and proliferation of satellite cells, respectively) in muscles of HFD mice, but these differences were not statistically significant (Fig. 2A). To document that satellite cell proliferation was unimpaired, we examined Brdu uptake on day 3 after injury. This measurement did not differ between mice fed the HFD and those fed the normal diet (Fig. 2B).

Desmin is an intermediate filament protein expressed during muscle differentiation; a decrease in desmin is

associated with impaired myofiber maturation (18). At 6 and 12 days after injury, desmin expression was significantly reduced in injured muscles of mice fed the HFD versus results from those fed the normal diet (Fig. 2C). To confirm these results, we assessed immunostaining of desmin in regenerating muscle. Desmin staining was reduced at both 6 and 12 days after injury (supplemental Fig. 2A), indicating that maturation of myofibers was impaired in regenerating muscle of HFD mice.

HFD impairs insulin/IGF-1 signaling in muscle and stimulates PTEN expression. We examined insulin/IGF-1 signaling in regenerating muscles at day 6 after injury when histologic differences were present in HFD compared with normal diet mice. In mice fed the normal diet, PIP_3 levels were increased in injured muscles compared with levels in uninjured muscles. Second, PIP_3 levels in both uninjured and injured muscles were reduced compared with results in muscles of mice fed the normal diet (Fig. 3A). The mechanism for the lower levels of PIP_3 associated with the HFD included suppression of IRS-1-associated PI3K activity in both uninjured and injured muscles compared with values in mice fed the normal diet (Fig. 3B). Besides reduced IRS-1-associated PI3K activity, PTEN expression was increased in both injured and uninjured muscles of HFD mice compared with results from mice fed the normal diet (Fig. 3C). The differences in PTEN expression were confirmed by immunostaining (supplemental Fig. 2B). Thus, at least two mechanisms could contribute to the HFD-induced decrease in PIP_3 in regenerating muscle: a decrease in IRS-1-associated PI3K activity and an increase in PTEN expression.

Palmitate impairs the growth of cultured myotubes, and PTEN deletion prevents it. In mice fed the HFD, impaired regeneration of injured muscles was associated with a lower level of PIP_3 . The latter could be attributed to both reduced production by IRS-1-associated PI3K and increased dephosphorylation by PTEN. Since the HFD raises circulating fatty acids (supplemental Fig. 1B), we examined their role in these responses. We treated primary cultures of myotubes with palmitate. At day 2 during the differentiation of myocytes to myotubes, we infected cells from PTEN (lox/lox) mice with Ad-Cre to knockout PTEN; infection with Ad- β -Gal served as the control. Infection with Ad-Cre decreased PTEN protein by >95% compared with infection with Ad- β -Gal (Fig. 4A).

Notably, deletion of PTEN was associated with an increase in myotube size compared with results from Ad- β -Gal-infected myotubes (Fig. 4B). The addition of palmitate to Ad- β -Gal-infected myotubes suppressed their growth, yielding smaller myotubes compared with results in myotubes not exposed to palmitate. PTEN deletion prevented the palmitate-induced decrease in cell size (Fig. 4B). To evaluate the influence of cell signaling on these cellular responses, we measured the phosphorylation of Akt and its downstream kinase, S6K1. As shown in Fig. 4C, palmitate treatment of Ad- β -Gal-infected cells decreased the levels of p-Akt and phosphorylated S6K1 (p-S6K1) compared with results from cells that were not treated with palmitate. PTEN deletion reversed the suppression of p-Akt and p-S6K1. These results indicate that palmitate, used to mimic the HFD, stimulated PTEN expression in muscle cells directly. Since PTEN knockout improved muscle cell growth, these results suggest that PTEN expression is responsible for the impaired maturation of muscle cells caused by an HFD.

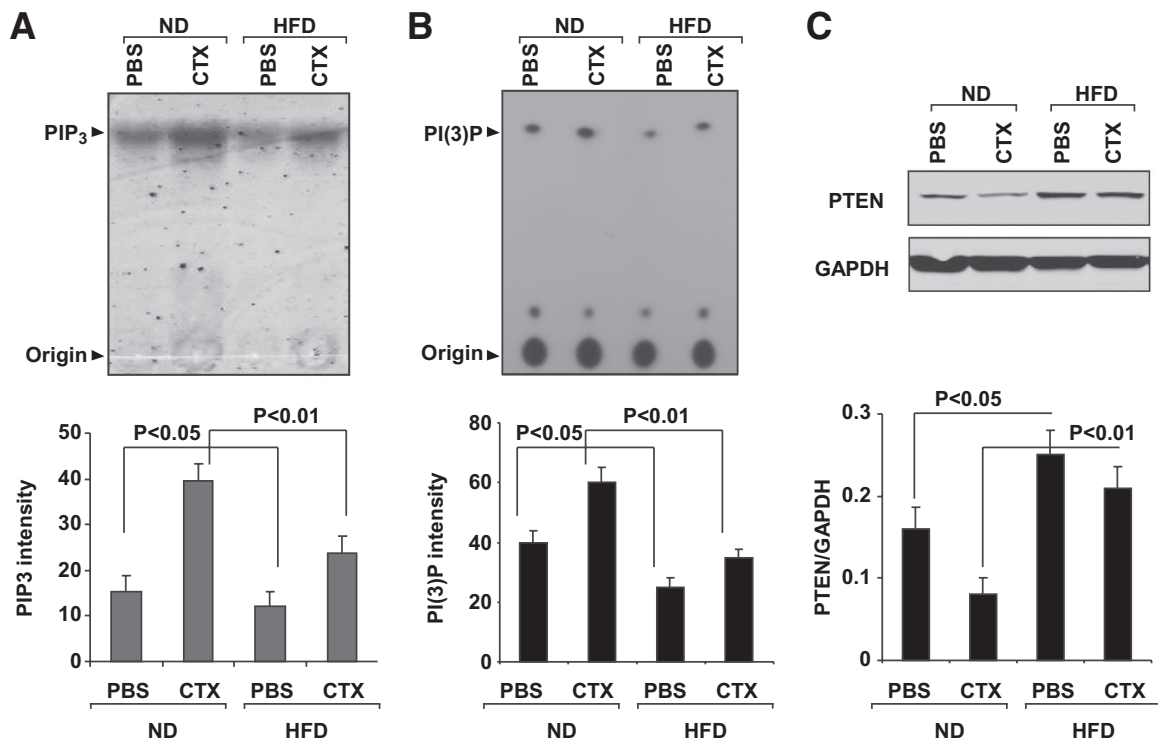


FIG. 3. HFD suppresses the accumulation of PIP₃ and IRS-1-associated PI3K activity in muscle during regeneration. **A:** At day 6 after injury, PIP₃ was increased in regenerating muscles of mice fed a normal diet (ND); the HFD reduced PIP₃ in uninjured and injured muscles ($n = 6$ in each group). **B:** In muscles of ND mice, IRS-1-associated PI3K activity was increased at day 6 after injury; the HFD significantly decreased this activity in uninjured and injured muscles ($n = 6$ in each group). **C:** In mice on a normal diet at 6 days after injury, Western blotting revealed a decrease in PTEN in regenerating myofibers. The HFD stimulated PTEN expression compared with results in mice on a normal diet ($n = 6$ in each group). CTX, cardiotoxin injury.

Muscle-specific PTEN knockout reverses HFD-induced impairment of muscle regeneration. To test conclusions obtained from results of treating cultured muscle cells with fatty acids (Fig. 4), we created MPKO mice. In muscles of these mice fed a normal diet, there was a marked decrease in PTEN compared with results from muscles of lox/lox mice (Fig. 5A). Based on immunostaining, we found that the small amount of PTEN found in muscle of MPKO mice was related to PTEN present in vascular or satellite cells (Fig. 5A).

In mice fed a normal diet, the weights of injured tibialis anterior muscles of MPKO mice were significantly greater than weights of tibialis anterior muscles from lox/lox mice (Fig. 5B). This result was confirmed by finding that regenerating myofibers were larger compared with the sizes of myofibers in injured muscles of lox/lox mice (Fig. 5C; supplemental Fig. 3A and B). In uninjured muscles, the levels of p-Akt and p-S6K1 in lox/lox mice were not different from those in MPKO mice (Fig. 5D and E). In injured muscles of MPKO mice, the levels of p-Akt and p-S6K1 were higher compared with results from lox/lox mice (Fig. 5D and E). These results indicate that with the normal diet, PTEN knockout promotes the regeneration of injured muscles.

After 8 months of the HFD, we found that muscle-specific knockout of PTEN improves several functions. First, blood glucose and insulin levels were lower compared with values in lox/lox mice ($P < 0.01$)—compatible with reduced insulin resistance as reported by Wijesekara et al. (19) (supplemental Fig. 1B). Second, the sizes of new myofibers from muscles of MPKO mice at days 6 and 12 after injury were larger compared with results from lox/lox mice (Fig. 6A; supplemental Fig. 3C and D), and the

weights of tibialis anterior muscles at days 12, 21, and 28 after injury were larger (Fig. 6B). Third, MPKO was associated with greater desmin expression in regenerating muscles at 6 and 12 days postinjury (Fig. 6C). Fourth, the increase in myofiber sizes of regenerating muscles in MPKO mice was associated with higher levels of p-Akt and its downstream mediator p-S6K1 (Fig. 6E). Finally, collagen deposition was reduced in regenerating muscles of HFD MPKO mice versus values in HFD lox/lox mice (Fig. 6D).

DISCUSSION

Diabetic patients can experience delayed healing of injured muscle or limited recovery from skeletal muscle infarction (20). To understand why the recovery of injured muscle becomes impaired, we studied the processes of muscle regeneration in a mouse model of insulin resistance achieved by HFD feeding for 8 months (14,19). The HFD led to smaller myofibers plus more collagen deposition in regenerating muscle (Fig. 1B and C). The unexpected finding was the absence of impaired satellite cell proliferation during muscle regeneration as assessed by BrdU incorporation or markers of impaired satellite cell activation or proliferation (Fig. 2A and B). One explanation for this finding is that suppression of the PI3K/Akt pathway impairs maturation of myotubes by mechanisms that are parallel to or downstream from MyoD or myogenin (21). We found that fatty acids directly impair the growth of cultured muscle cells, leading to the conclusion that the HFD-induced increase in circulating fatty acids interferes with myofiber maturation and growth but not activation of satellite cell function.

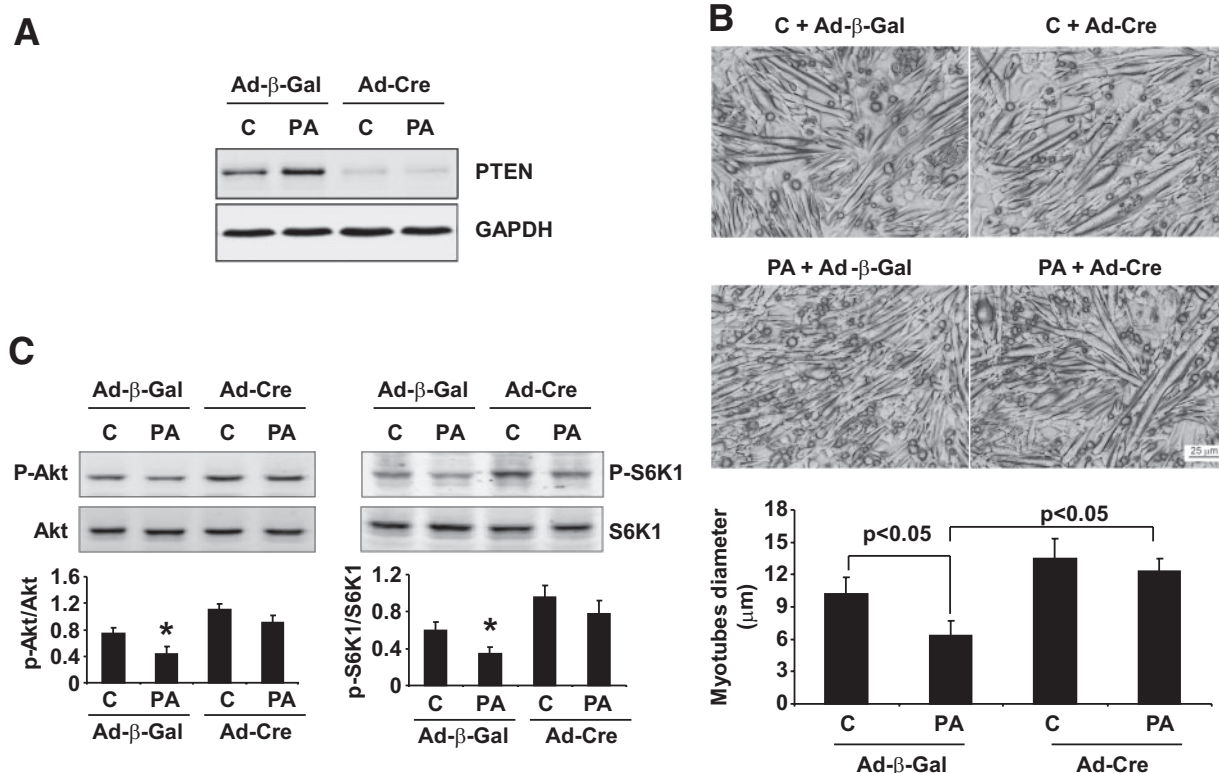


FIG. 4. Palmitate impairs the growth of cultured myotubes, and PTEN deletion prevents it. **A:** Primary cultures of muscle cells from $PTEN^{lox/lox}$ Cre^{-} mice were infected by adenoviruses: Ad-Cre to delete PTEN or Ad-β-Gal (control). Infected cells were then treated with palmitate (PA) or vehicle (C), and the expression of PTEN was evaluated by Western blot using GAPDH as the loading control. **B:** Cultured muscle cells from **A** were examined for difference in myotube diameters. **C:** Phosphorylation of Akt and S6K1 was evaluated in muscle cell cultures from **A**. The ratios of p-Akt/Akt (Ser473) and p-S6K1/S6K1 (Thr389) were calculated for three separate experiments.

How do fatty acids impair muscle cell growth? Other investigators have suggested that impaired muscle growth during regeneration could be linked to defects in insulin/IGF-1 signaling. For example, muscle-specific IGF-1 overexpression has been shown to enhance muscle regeneration in several conditions (22–24). Our results revealed that PIP_3 levels were significantly lower in regenerating muscles of HFD mice compared with those in mice fed the normal diet (Fig. 3A). One mechanism for the lower PIP_3 level in muscle of HFD mice was impaired activity of IRS-1-associated PI3K (Fig. 3B). We uncovered an alternative mechanism: an increase in PTEN expression would dephosphorylate and inactivate PIP_3 , and this could determine the responses to other growth factors or hormones that improve muscle regeneration by raising the level of PIP_3 (3).

In exploring mechanisms for the association between a low PIP_3 level and impaired muscle regeneration, we found that fatty acids directly stimulate cultured muscle cells to express PTEN. The fatty acid-induced increase in PTEN in cultured muscle cells would decrease PIP_3 , leading to decreased phosphorylation of Akt and S6K1 and suppressed cell growth. To examine whether the PIP_3 pathway also is involved in vivo, we studied mice with increased circulating fatty acids from eating the HFD. In uninjured or injured muscles of HFD mice, the expression of PTEN was increased compared with results in mice fed a normal diet (Fig. 3C). Interestingly, PTEN expression in injured muscles of mice fed a normal diet was reduced compared with results in uninjured muscle (Fig. 3C). This result might be explained by the inflammation that is stimulated by muscle injury given that nuclear fac-

tor- κ B activation can decrease PTEN expression in muscle (25,26). Therefore, the increased PTEN expression in injured muscle of HFD mice reflects a stronger response to the HFD-induced increase in circulating fatty acids.

Since fatty acids act to stimulate PTEN expression in muscle cells and reduce their growth, we examined potential mechanisms for these responses (Fig. 4B). Application of palmitate to muscle cells not only increased PTEN expression but also reduced the levels of p-Akt and p-S6K1 (Fig. 4C). These changes would be associated with a decrease in muscle protein because of stimulated protein degradation by the ubiquitin-proteasome system and suppressed protein synthesis (27–29). When we deleted PTEN in muscle cells, there was resistance to the defects caused by free fatty acids (Fig. 4B). To confirm these results, we examined the importance of PTEN in vivo by creating mice with muscle-specific knockout of PTEN. In MPKO mice fed the HFD, defects in muscle maturation and the small size were eliminated (Fig. 6).

In addition to the impaired muscle regeneration, the HFD led to collagen accumulation in injured muscles (Fig. 1D). A mechanism for this finding could be linked to the HFD-induced increase in blood glucose (supplemental Fig. 1B) because hyperglycemia can stimulate collagen deposition (17,30). Alternatively, the HFD might activate cytokine release to raise transforming growth factor- β , which can stimulate fibrosis (31). As with the HFD-induced defects in muscle regeneration, collagen deposition was markedly suppressed in mice with muscle-specific PTEN deletion (Fig. 6D).

In conclusion, we find that an HFD raises circulating

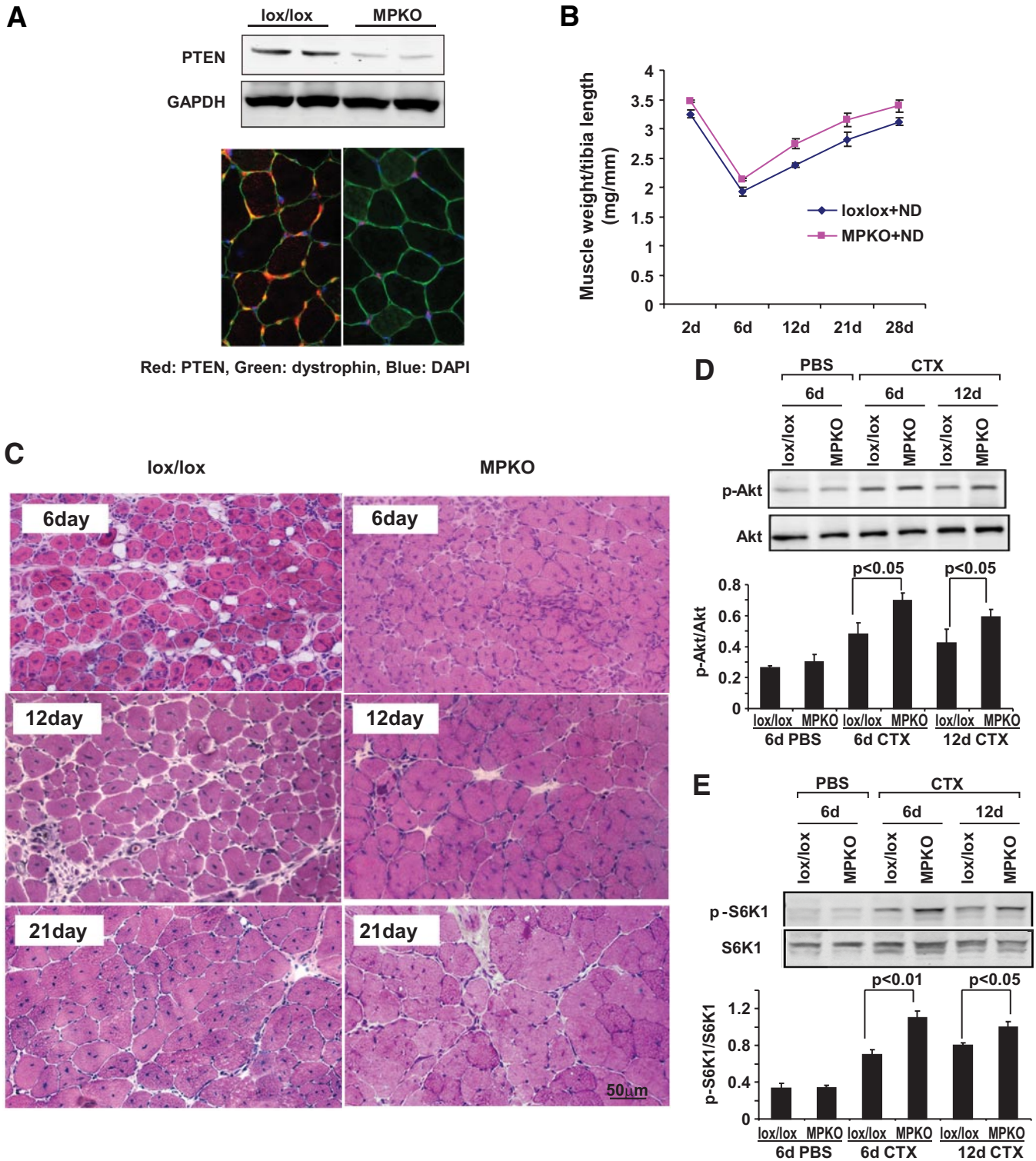


FIG. 5. Muscle-specific PTEN deletion (MPKO) improved muscle regeneration in 3-month-old mice fed a normal diet. **A:** PTEN protein was markedly decreased in MPKO muscles vs. control lox/lox mice as assessed by Western blot (*upper panel*). PTEN (red) immunostaining (*lower panel*) was absent in myofibers of MPKO mice but was present in vascular or satellite cells (arrow). Green, dystrophin. Blue, DAPI. **B:** The weight of tibialis anterior muscles (factored by tibia length) after injury was improved in MPKO mice fed a normal diet compared with that in HFD mice ($n = 6$ in each group). **C:** Hematoxylin-eosin staining of tibialis anterior injured muscles in MPKO mice fed a normal diet revealed larger myofibers with central nuclei compared with responses in lox/lox mice. **D:** At 6 and 12 days after cardiotoxin (CTX) injury, the ratio of p-Akt/Akt (Ser473) was significantly higher in muscle of MPKO vs. lox/lox mice. Both groups were fed the normal diet ($P < 0.05$; $n = 6$ in each group). **E:** the increase in p-Akt was associated with an increase in p-S6K1 (Thr389). Total S6K1 was used as loading control ($P < 0.05$; $n = 6$ in each group). * $P < 0.05$, d, days. (A high-quality digital representation of this figure is available in the online issue.)

fatty acids, which interfere with muscle regeneration through mechanisms involving impaired myofiber maturation. There was no impairment of the capacity of satellite

cells to proliferate. The mechanism for the decrease in maturation is initiated by a direct effect of fatty acids, which increases PTEN expression in muscle and impairs

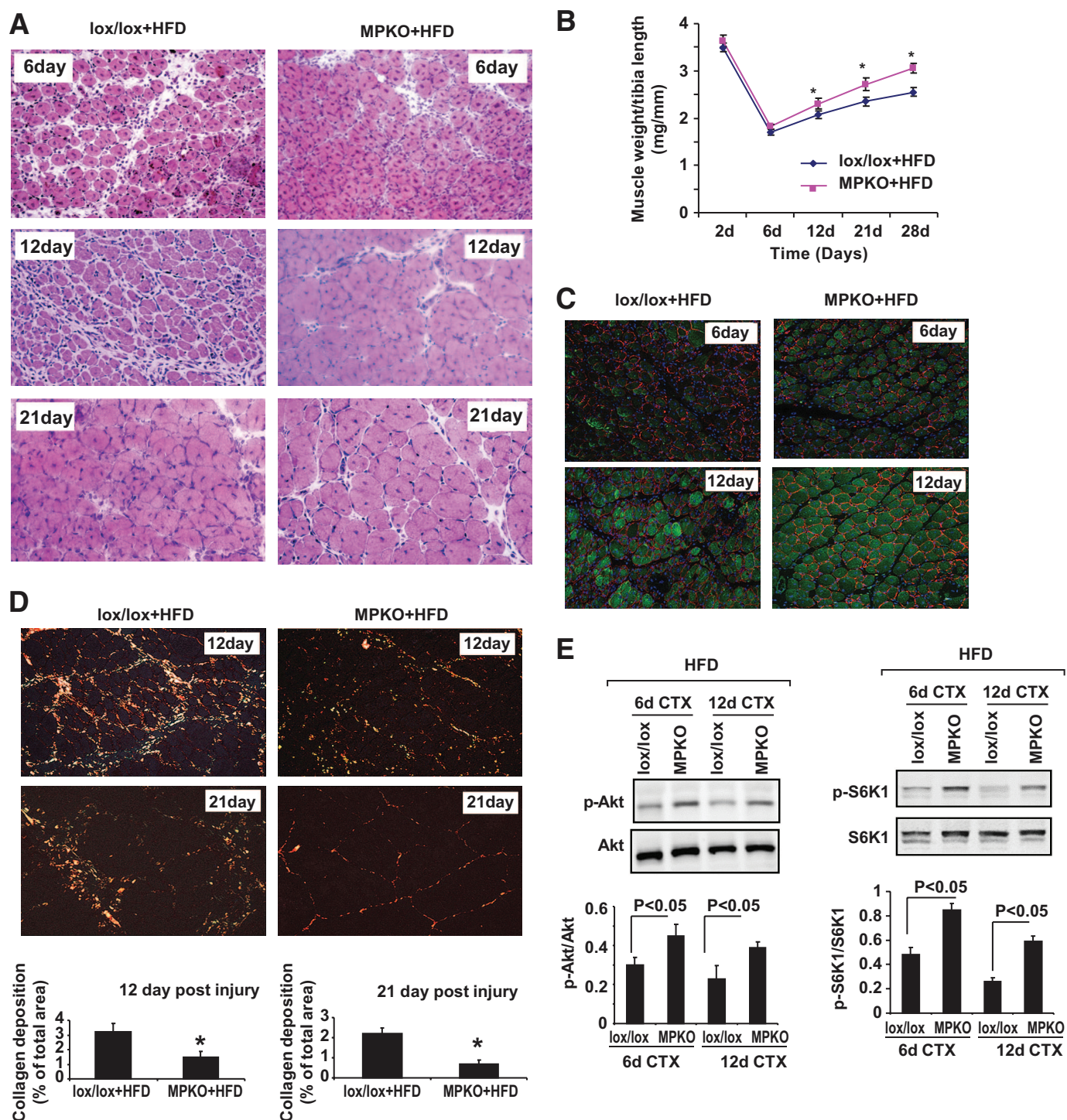


FIG. 6. In HFD mice with muscle-specific PTEN deletion (MPKO), the suppression of myofiber maturation and the increase in collagen deposition were blocked. **A:** Hematoxylin-eosin staining revealed improved maturation of myofibers in injured tibialis anterior muscles of MPKO HFD mice (*right panel*) compared with results in muscles of HFD control lox/lox mice (*left panel*). **B:** MPKO improved weight gain of injured tibialis anterior muscles factored for tibia length compared with results from lox/lox HFD mice ($n = 12$ in each group). $*P < 0.01$. **C:** At 6 and 12 days after injury, immunostaining of the differentiation marker, desmin, increased in injured muscles of MPKO mice fed the HFD (*right panel*) at 6 and 12 days after injury compared with results in HFD control lox/lox mice (*left panel*). **D:** At days 12 and 21 after injury, Sirius red staining for collagen in muscles of HFD MPKO mice (*right panel*) revealed a significant reduction vs. results in muscles of HFD lox/lox mice (*left panel*). Bar graphs (*lower panel*) represent the fractions of injured muscle staining for collagen. $n = 6$. $*P < 0.05$. **E:** The ratio of p-Akt/Akt (Ser473) in muscle of lox/lox mice fed the HFD was lower than in muscle of MPKO mice ($n = 6$ in each group). The ratio of p-S6K1/S6K1 (Thr389) had a similar pattern ($n = 6$ in each group). CTX, cardiotoxin injury. (A high-quality digital representation of this figure is available in the online issue.)

muscle cell growth. A critical role of PTEN in these HFD-induced defects was documented in studies showing that PTEN deletion blocked the impaired growth of muscle cells, the abnormalities in regeneration of injured

muscle, and the increased deposition of collagen. If similar pathways occur in diabetic patients, therapeutic strategies directed at improving the repair of damaged muscle could include suppression of PTEN activity.

ACKNOWLEDGMENTS

The work was supported by National Institutes of Health grants R37 DK37175, P50 DK64233, and R01 DK62828. H.W. was supported by Shanghai Science and Technology Commission (STC) Grant 07QH14020.

No potential conflicts of interest relevant to this article were reported.

REFERENCES

- Hirsch T, Spielmann M, Velander P, Zuhaili B, Bleiziffer O, Fossum M, Steinstraesser L, Yao F, Eriksson E. Insulin-like growth factor-1 gene therapy and cell transplantation in diabetic wounds. *J Gene Med* 2008;10:1247–1252
- Vignaud A, Ramond F, Hourde C, Keller A, Butler-Browne G, Ferry A. Diabetes provides an unfavorable environment for muscle mass and function after muscle injury in mice. *Pathobiology* 2007;74:291–300
- Shortreed K, Johnston A, Hawke TJ. Satellite cells and muscle repair. In *Skeletal Muscle Damage and Repair*. 1st ed. Tiidus PM, Ed. Champaign, IL, Human Kinetics, 2008, p. 77–88
- Grefte S, Kuijpers-Jagtman AM, Torensma R, Von den Hoff JW. Skeletal muscle development and regeneration. *Stem Cells Dev* 2007;16:857–868
- Charge SB, Rudnicki MA. Cellular and molecular regulation of muscle regeneration. *Physiol Rev* 2004;84:209–238
- Barton ER, Morris L, Musaro A, Rosenthal N, Sweeney HL. Muscle-specific expression of insulin-like growth factor 1 counters muscle decline in mdx mice. *J Cell Biol* 2002;157:137–147
- Musaro A, McCullagh K, Paul A, Houghton G, Dobrowolny G, Molinaro M, Barton ER, Sweeney HL, Rosenthal N. Localized IGF-1 transgene expression sustains hypertrophy and regeneration in senescent skeletal muscle. *Nat Genet* 2001;27:195–200
- Song Y-H, Li Y, Du J, Mitch WE, Rosenthal N, Delafontaine P. Muscle-specific expression of insulin-like growth factor-1 blocks angiotensin II-induced skeletal muscle wasting. *J Clin Invest* 2005;115:451–458
- Zhang L, Wang XH, Wang H, Hu Z, Du J, Mitch WE. Satellite cell dysfunction and impaired IGF-1 signaling cause CKD-induced muscle atrophy. *J Am Soc Nephrol* 2010;21:419–427
- Lai KM, Gonzalez M, Poueymirou WT, Kline WO, Na E, Zlotchenko E, Stitt TN, Economides AN, Yancopoulos GD, Glass DJ. Conditional activation of Akt in adult skeletal muscle induces rapid hypertrophy. *Mol Cell Biol* 2004;24:9295–9304
- Wang XH, Du J, Klein JD, Bailey JL, Mitch WE. Exercise ameliorates chronic kidney disease-induced defects in muscle protein metabolism and progenitor cell function. *Kidney Int* 2009;76:751–759
- Hu Z, Lee IH, Wang X, Shang H, Zhang L, Du J, Mitch WE. PTEN expression contributes to the regulation of muscle protein degradation in diabetes. *Diabetes* 2007;56:2449–2456
- d'Albis A, Couteaux R, Janmot C, Roulet A, Mira JC. Regeneration after cardiotoxin injury of innervated and denervated slow and fast muscles of mammals: myosin isoform analysis. *Europ J Biochem* 1988;174:103–110
- Hu J, Klein JD, Du J, Wang XH. Cardiac muscle protein catabolism in diabetes mellitus: activation of the ubiquitin-proteasome system by insulin deficiency. *Endocrin* 2008;149:5384–5390
- Bruning JC, Michael MD, Winnay JN, Hayashi T, Horsch D, Accili D, Goodyear LJ, Kahn CR. A muscle-specific insulin receptor knockout exhibits features of the metabolic syndrome of NIDDM without altering glucose tolerance. *Mol Cell* 1998;2:559–569
- Tschope C, Walther T, Koniger J, Spillmann F, Westermann D, Escher F, Pauschinger M, Pesquero JB, Bader M, Schultheiss HP, Noutsias M. Prevention of cardiac fibrosis and left ventricular dysfunction in diabetic cardiomyopathy in rats by transgenic expression of the human tissue kallikrein gene. *FASEB J* 2004;18:828–835
- Berria R, Wang L, Richardson DK, Finlayson J, Belfort R, Pratipanawat T, De Filippis EA, Kashyap S, Mandarino LJ. Increased collagen content in insulin-resistant skeletal muscle. *Am J Physiol* 2006;290:E560–E565
- Hawke TJ, Meeson AP, Jiang N, Graham S, Hutcheson K, DiMaio JM, Garry DJ. p21 is essential for normal myogenic progenitor cell function in regenerating skeletal muscle. *Am J Physiol Cell Physiol* 2003;285:C1019–C1027
- Wijesekara N, Konrad D, Eweida M, Jefferies C, Liadis N, Giacca A, Crackower M, Suzuki A, Mak TW, Kahn CR, Klip A, Woo M. Muscle-specific Pten deletion protects against insulin resistance and diabetes. *Mol Cell Biol* 2005;25:1135–1145
- Madhan KK, Symmans P, Te SL, van Der MW. Diabetic muscle infarction in patients on dialysis. *Am J Kidney Dis* 2000;35:1212–1216
- Wilson EM, Tureckova J, Rotwein P. Permissive roles of phosphatidylinositol 3-kinase and Akt in skeletal myocyte maturation. *Mol Biol Cell* 2004;15:497–505
- Pelosi L, Giacinti C, Nardis C, Borsellino G, Rizzuto E, Nicoletti C, Wannenes F, Battistini L, Rosenthal N, Molinaro M, Musaro A. Local expression of IGF-1 accelerates muscle regeneration by rapidly modulating inflammatory cytokines and chemokines. *FASEB J* 2007;21:1393–1402
- Rabinovsky ED, Gelir E, Gelir S, Lui H, Kattash M, DeMayo FJ, Shenaq SM, Schwartz RJ. Targeted expression of IGF-1 transgene to skeletal muscle accelerates muscle and motor neuron regeneration. *FASEB J* 2003;17:53–55
- Mourkioti F, Kratsios P, Luedde T, Song YH, Delafontaine P, Adami R, Parente V, Bottinelli R, Pasparakis M, Rosenthal N. Targeted ablation of IKK2 improves skeletal muscle strength, maintains mass, and promotes regeneration. *J Clin Invest* 2006;116:2945–2954
- Zhang L, Ran L, Garcia GE, Wang XH, Han S, Du J, Mitch WE. Chemokine CXCL16 regulates neutrophil and macrophage infiltration into injured muscle, promoting muscle regeneration. *Am J Pathol* 2009;185:2518–2527
- Vasudevan KM, Gurumurthy S, Rangnekar VM. Suppression of PTEN expression by NF- κ B prevents apoptosis. *Mol Cell Biol* 2004;24:1007–1021
- Hu Z, Wang H, Lee IH, Du J, Mitch WE. Endogenous glucocorticoids and impaired insulin signaling are both required to stimulate muscle wasting under pathophysiological conditions in mice. *J Clin Invest* 2009;119:7650–7659
- Lecker SH, Goldberg AL, Mitch WE. Protein degradation by the ubiquitin-proteasome pathway in normal and disease states. *J Am Soc Nephrol* 2006;17:1807–1819
- Wang XH, Hu Z, Hu JP, Du J, Mitch WE. Insulin resistance accelerates muscle protein degradation: activation of the ubiquitin-proteasome pathway by defects in muscle cell signaling. *Endocrin* 2006;147:4160–4168
- Han DC, Isono M, Hoffman BB, Ziyadeh FN. High glucose stimulates proliferation and collagen type I synthesis in renal cortical fibroblasts: mediation by autocrine activation of TGF- β . *J Am Soc Nephrol* 1999;10:1891–1899
- Jiang T, Wang XX, Scherzer P, Wilson P, Tallman J, Takahashi H, Li J, Iwahashi M, Sutherland E, Arend L, Levi M. Farnesoid X receptor modulates renal lipid metabolism, fibrosis, and diabetic nephropathy. *Diabetes* 2007;56:2485–2493